Monthly Weather Review

VOLUME 99, NUMBER 12

DECEMBER 1971

UDC 551.558.2:551.511.2

NUMERICAL SIMULATION OF THE LIFE CYCLE OF A THUNDERSTORM CELL

YOSHIMITSU OGURA and TSUTOMU TAKAHASHI [1]

Laboratory for Atmospheric Research, University of Illinois, Urbana, Ill.

ABSTRACT

A model of cumulus clouds is presented that combines the vertical equation of motion, the equation of mass continuity, the first law of thermodynamics, and the following cloud microphysical processes: condensation of water vapor to produce cloud droplets, conversion of cloud droplets to raindrops, glaciation, sublimation of water vapor, melting of ice crystals, evaporation of cloud droplets, evaporation of raindrops, evaporation of ice crystals, and evaporation of melting ice crystals. The conversion and glaciation processes are parameterized and the drag force is assumed to be provided by the weight of hydrometeors.

The result of time integration of the model shows that, with the inclusion of the microphysical processes, some aspects of the three stages of the life cycle of a cumulus cloud as depicted by Byers and Braham in 1949 (developing stage, mature stage, and decaying stage) are simulated qualitatively by the model. The model also shows that the rate of conversion from cloud droplets to raindrops is important in determining the duration of the life cycle of a thunderstorm cell. This is exemplified in a case with a small rate of conversion where a thunderstorm cell is maintained in a steady state despite the drag force due to a large number of hydrometeors. Also investigated is the relative importance of various microphysical processes in determining dynamic as well as thermodynamic behavior of a cloud during the entire life cycle.

1. INTRODUCTION

This article will report the results of our first effort to numerically simulate some aspects of the life cycle of an individual thunderstorm cell and to investigate the interaction between dynamical and microphysical processes involved. The numerical model to be presented here combines the vertical equation of motion, the equation of mass continuity, the first law of thermodynamics and a number of cloud microphysical processes.

One of the first attempts to simulate numerically the evolution of moist convection was made by one of the authors (Ogura 1963*b*) [2] with axisymmetric simplifications. The full equations of motion and thermodynamics were integrated numerically on a space grid as an initial value problem. His study was based on the anelastic equations derived by Ogura and Phillips (1962) for reversible processes and, therefore, it ignored the fallout of precipitation water. Asai (1964) and Orville (1965) also ignored the rainfall process in their two-dimensional modeling of cumulus convection. On the other hand, Das (1964) and Takeda (1966*a*, 1966*b*) incorporated the rainfall process into a two-dimensional model, evaporation being taken into account.

In contrast to these approaches, Kessler (1967) prescribed the air flow inside a cloud and considered the changes of hydrometeors with time.[3] He simplified the cloud microphysics calculations by reducing them to a series of parameterized relationships. Srivastava (1967) used Kessler's parameterization and showed that the development of raindrops is an important factor in the decay of isolated cumuli. Arnason et al. (1968, 1969) and Murray (1970) extended this type of treatment to two-dimensional convection and Orville (1968), Liu and Orville (1969), and Orville and Sloan (1970) extended it to mountain-induced cumuli. Takeda (1971) recently presented a more sophisticated two-dimensional model where the size distribution of water drops was described by using seven discrete radii. Simpson and Wiggert (1969, 1971) and Weinstein (1970) added the freezing process in their one-dimensional modeling.

In our model, the following microphysical processes will be considered: condensation of water vapor to produce cloud droplets, conversion of cloud droplets to raindrops, glaciation, sublimation of water vapor, melting of ice

[1] Present address: Cloud Physics Observatory, University of Hawaii, Hilo.

[2] A survey article by Ogura (1963*a*) describes in detail the earlier results of numerical simulation of small scale and mesoscale atmospheric convection.

[3] His works along this line have been collected in one report (Kessler 1969).

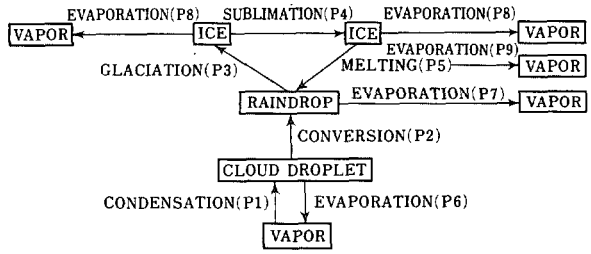

FIGURE 1.—Scheme of cloud microphysical processes in a thunderstorm.

crystals, evaporation of cloud droplets, evaporation of raindrops, evaporation of ice crystals, and evaporation of ice crystals in the process of melting. Figure 1 shows schematically the transformation between various phases of water substance.

The motivation of this study came from many sources. First came the increasingly widespread interest in cloud modification experiments (e.g. Rand Corporation 1969). Undoubtedly good modeling of cumulus clouds is of great value for designing and evaluating results of field experiments of cloud modification (Simpson and Wiggert 1969, 1971, and Weinstein 1970).

Proper incorporation of cumulative effects of cumulus type convection into a model is also essential for the success of numerical modeling of the general circulation of the atmosphere and, in particular, of the tropical circulation. Recent investigation revealed that cloud clusters occurring over all tropical oceans and practically all seasons appear to be major contributors to the energy release in the atmosphere over tropical oceans. Each cloud cluster consists of a number of mesoconvective-scale cells with characteristic dimensions of the order of 10 to 100 km, and several cumulonimbus towers tend to be organized to form such a mesoconvective-scale cell (WMO–ICSU 1970). Therefore, one must describe the behavior of cumulonimbus clouds in terms of parameters associated with larger scale motions.

The recent studies on numerical simulation of an isolated cumulus cloud referred to above clearly indicate that the inclusion of microphysical processes is important to successful simulation of the dynamical behavior of cumulus clouds. The importance of the interaction between dynamical and microphysical processes was also emphasized by Mason (1969) in his excellent review paper on some outstanding problems in cloud physics; the growth and fallout processes of precipitation interact with the updraft, which in turn controls the amount and development of hydrometeors.

No serious attempts are made in this article to simulate real clouds. The primary purpose of this article is rather to estimate the importance of various microphysical processes in the life cycle of a thunderstorm cell.

2. MICROPHYSICAL PROCESSES

CONDENSATION PROCESS

Supersaturation in clouds is estimated to be below 0.4 percent even when the updraft is 4 m/s (Howell 1949). Our model, therefore, assumes that all water vapor over the saturation level condenses instantaneously into small cloud droplets. The actual procedure for calculating the rate of condensation of water vapor per unit time (P1) is given in section 4.

In our simplified model, liquid water is divided into two parts, cloud droplets and raindrops. It is not necessary to specify the size distribution of cloud droplets. However, the typical size of cloud drops is in the range of 10–20 μm, as was observed by Weickmann and aufm Kampe (1953), Warner (1969) and others, so that cloud droplets are assumed to share the motion of the air in all aspects.

CONVERSION PROCESS FROM CLOUD DROPLETS TO RAINDROPS

After the water vapor is condensed to form cloud droplets, a process that we call conversion begins, through which small cloud droplets are converted into large raindrops. Normal condensation growth tends to create a narrow dropsize spectrum. Several explanations have been given to account for the fast broadening of the size spectrum, such as those observed by Durbin (1959) and Warner (1969), ranging from stochastic collisions between many small droplets (Golovin 1963, Berry 1967, 1968) to the influence of weak electric fields (Semonin and Plumlee 1966, Sartor 1967). At the present time, however, there is no completely accepted explanation.

As soon as some raindrops have been produced by autoconversion or coalescence, raindrops begin to fall with different velocities depending upon their sizes. In the course of this fall, they are envisaged to collect cloud droplets through the continuous collection process described by Langmuir (1948). The rate of growth of an individual drop by this process is proportional to the mixing ratio of cloud droplets.

On the other hand, we know that the size distribution of raindrops is well represented by the following inverse exponential law not only for rain observed at the earth's surface (Marshall and Palmer 1948) but also in the free atmosphere (Caton 1966):

$$n=n_0e^{-\lambda D} \tag{1}$$

where D is the diameter of a raindrop, n is the number of drops per unit volume in the size interval delineated by D and $D+dD$, and n_0 and λ are constants which are determined empirically. This may indicate that the effects of autoconversion, collection, and evaporation, which act to change the form of the size-distribution, are ballanced so that the size-distribution is in approximate accord with the Marshall-Palmer distribution.

In this study, we use a parameterization that does not depend upon the details of how autoconversion and collection are achieved, but it simply states that the conversion from cloud droplets to raindrops is achieved at a given rate and that the rate, P2, is proportional to the mixing ratio of cloud droplets. P2 is then written as

$$\mathrm{P2}=\left(\frac{dQ_r}{dt}\right)_{\mathrm{conv.}}=CoQ_c \tag{2}$$

where t denotes time, Q_c and Q_r are the mixing ratios of cloud droplets and raindrops, respectively, in gm/gm. The parameter Co may be regarded as the reciprocal of the "conversion time" of the cloud droplets. As will be seen later, values of Co in the range of 0–0.2 were used in this study. A typical value of 0.005 corresponds to 3.5 min of conversion time.

At this point, we should mention that the following autoconversion equations (in our notations) were proposed by Kessler (1969) and Berry (1968) respectively:

$$\frac{dQ_r}{dt}\,(\text{autoconversion})=k_1(Q_c-b), \qquad Q_c>b \tag{3}$$

and

$$\frac{dQ_r}{dt}\,(\text{autoconversion})=\frac{10^6(\rho_{a0}Q_c)^2}{60\left(5\rho_{a0}+\dfrac{0.0366}{10^6Q_c}\cdot\dfrac{N_b}{D_b}\right)}. \tag{4}$$

The typical values suggested by Kessler for the parameters k_1 and b are $k_1=10^{-3}$ s^{-1} and $b=5\times10^{-4}$ gm/gm. In eq (4), ρ_{a0} denotes the environmental air density (gm·cm^{-3}). Simpson and Wiggert (1969) used D_b (spectrum dispersion)$=0.366$ and N_b (particle concentration at cloud base)$=50$ cm^{-3} as typical values for maritime clouds. When $Q_c=10^{-3}$ gm/gm and $\rho_{a0}=10^{-3}$ gm·cm^{-3}, eq (3) gives $dQ_r/dt=0.5\times10^{-6}$ gm·gm^{-1}·s^{-1} and eq (4) gives 1.7×10^{-6} gm·gm^{-1}·s^{-1}.

Kessler also proposed the following collection equation:

$$\frac{dQ_r}{dt}\,(\text{collection})=k_2Q_cQ_r^{0.875} \tag{5}$$

The typical value for the parameter k_2 is 2.19 in our units. When $Q_c=Q_r=10^{-3}$ gm/gm, eq (3) combined with eq (5) gives, therefore, 5.8×10^{-6} gm·gm^{-1}·s^{-1} as the rate of conversion from cloud droplets to raindrops, and eq (4) combined with eq (5) gives 7.0×10^{-6} gm·gm^{-1}·s^{-1}, whereas eq (2) with $Co=5\times10^{-3}$ gives 5×10^{-6} gm·gm^{-1}·s^{-1}.

The collision efficiency is a key factor in calculating the growth of cloud droplets and raindrops. The theoretical values presented by Hocking (1959) and Shafrir and Neiburger (1963) have been widely used in such calculations. However, the experimental results obtained by Telford et al. (1955), Schotland (1957), Woods and Mason (1965) and Steinberger et al. (1968) indicate that the collision efficiency between particles of nearly equal sizes is high. Also, a high collision efficiency was obtained between big drops (≈130 μm) and small droplets (≈8 μm) by Beard and Pruppacher (1971). Recently, Davis and Sartor (1967) and Hocking and Jonas (1970) refined the collision efficiency for small droplets (<30 μm). A further refinement of calculations of the collision efficiency, especially for droplets larger than 30 μm, may be needed. We may also refer to experimental studies on the interaction between two equal-sized particles [Eveson et al. (1959), Happel and Pfeffer (1960)]. A study of the charge generation mechanism may also be necessary because the coalescence efficiency depends upon the electric charge of drops (Semonin and Plumlee 1966, Sartor 1967). In the present article, we are contented with using the very simplified eq (2).

In this study, we must evaluate a representative (mean volume-weighted) terminal velocity of raindrops, V_w, in terms of the raindrop content. This may be given as a ratio of the vertical flux of raindrops (F in gm·cm^{-2}·s^{-1}) to the liquid water content (l_r in gm·cm^{-3}):

$$V_w=\frac{F}{l_r}. \tag{6}$$

In this expression, l_r and F are defined as

$$l_r=\int_0^\infty nmdD \tag{7}$$

and

$$F=\int_0^\infty nmvdD \tag{8}$$

where m is the mass of a liquid drop and v is the terminal velocity of the drop. According to Kessler (1969), v is given as a function of D as

$$v=v_0D^{1/2} \tag{9}$$

with $v_0=1{,}300$ when v is measured in cm/s and D in cm. With the assumption that n is expressed as a function of D by the Marshall-Palmer distribution [eq (1)], l_r and F are given by

$$l_r=\int_0^\infty ne^{-\lambda D}\frac{\pi}{6}\rho_wD^3dD=\frac{\pi\rho_w}{\lambda^4}n_0 \tag{10}$$

and

$$F=\left(\frac{\pi}{6}\right)\Gamma\left(\frac{9}{2}\right)\rho_wv_0n_0\lambda^{-9/2} \tag{11}$$

where ρ_w is the density of liquid water and Γ represents the Gamma function. Eliminating λ between these two equations, we have the following relation between l_r and F:

$$F=\frac{1}{6}\pi^{-1/8}\Gamma\left(\frac{9}{2}\right)\rho_w^{-1/8}v_0n_0^{-1/8}l_r^{9/8}. \tag{12}$$

We shall then use the empirical relation that the liquid water content of 1 gm·m^{-3} corresponds approximately to the precipitation intensity of 20 mm/hr (Blanchard 1953). Equation (12) is then transformed to give

$$F=\frac{1}{1.8}10^{15/4}l_r^{9/8} \tag{13}$$

and, consequently,

$$V_w=3.12\times10^3\,(\rho_aQ_r)^{0.125}\ (\text{cm/s}) \tag{14}$$

where ρ_a is the density of dry air. This equation gives 5.56 m/s as the falling speed for a water content of 10^{-3} gm·cm^{-3}.

It may be noted that the following equation was derived by Kessler (1969) and used by Simpson and Wiggert (1969, 1971) and Weinstein (1970) in their cumulus modeling studies:

$$V_w=2.91\times10^3\,(\rho_aQ_r)^{0.125}. \tag{15}$$

This equation can be derived from eq (12), but with the empirical value of $n_0=10^{-1}$ cm^{-4}. The difference between the values of V_w given by eq (14) and (15) is only a few percent. Liu and Orville (1969) used a slightly different equation for V_w. Their equation gives 5.32 m/s as the falling speed for a water content of 10^{-3} gm·cm^{-3}, again very close to that given by eq (14).

GLACIATION PROCESS

The present knowledge of the glaciation process appears not to be sufficient to warrant a serious attempt to simulate this process in detail. For example, the forms or habits of the ice crystals are not well documented, though much progress has been made recently in this area (e.g., Mossop and Ono 1969). Ice nuclei had been thought to determine the concentration of ice crystals. However, Koenig (1963), Braham (1964), Mossop (1968), and Hobbs (1969) reported that the number of ice crystals was three orders higher than the number of ice nuclei at a temperature near freezing. By observing the transition from liquid phase to solid phase, Koenig (1963) found that 2 min was sufficient time to transform the liquid phase to solid phase.

The uncertainty remains also in collection efficiencies of ice crystals. Laboratory results of Hosler and Hallgren (1960) suggest that ice crystal collection efficiencies may be much less than those of raindrops, whereas Weickmann (1957) indicated that the protuberances of snow particles may enhance their collection efficiencies above those of raindrops. Fletcher (1962) calculated the collection efficiency of an ice disk falling through droplets. He points out, however, that there is no general agreement as to the correctness of these values.

Due to the uncertainties described, we use in this study a parameterization that simply states that the glaciation process takes place whenever the air temperature is below the freezing point and the rate of production of ice crystals, P3, is proportional to the mixing ratio of raindrops, Q_r. P3 is then given by

$$\mathrm{P3}=\left(\frac{dQ_i}{dt}\right)_{\mathrm{glac}}=GQ_r \tag{16}$$

where Q_i is the mixing ratio of ice particles. The parameter G may be regarded as the reciprocal of the "glaciation time" of raindrops and was assigned values in the range of 0–0.05. In this simplified model, the nucleation of snow crystals from cloud droplets is not considered. In other words, cloud droplets are assumed to remain in liquid phase even at temperatures below the freezing point (see section 8 for further discussion).

For ice particles, the terminal velocity may be expressed as

$$v=v_0D^{1/2}f_0 \tag{17}$$

where f_0 is 0.75 for hailstones and 0.37 for graupel pellets (Byers 1965). Following the same procedure as above, the representative terminal velocity for ice particles, V_i, is given by

$$V_i=3.12\times10^3\ (\rho_aQ_i)^{0.125}f_0.\ \text{(cm/s)} \tag{18}$$

Throughout this study, f_0 is 0.75.

In some of the cases in this series of numerical experiments, however, we assume that ice crystals take the form of snowflakes in the layer where air temperature is below the freezing point. In such cases, the size-distribution of snowflakes is assumed to follow the Gunn-Marshall distribution (Gunn and Marshall 1958). The relation between F and l_r in this case is given by

$$F=2.13\times10^3\ (l_r)^{1.11} \tag{19}$$

where the fall velocity of a snowflake is assumed to be a function of the diameter D (cm) expressed as

$$v=200\mathrm{D}^{0.31}. \tag{20}$$

The representative terminal velocity for snowflakes is

$$V_i=5.92\times10^2\ (\rho_aQ_i)^{0.11}.\ \text{(cm/s)} \tag{21}$$

SUBLIMATION PROCESS

It is assumed that water vapor sublimates to ice crystals when the air temperature is below the freezing point and water vapor exceeds the saturation water vapor for a plane ice surface. The rate of growth of an ice crystal, P4, by the sublimation process may depend upon the forms of the ice crystals. With the assumption that ice crystals are spheres, the combination of the sublimation formula (Mason 1957) with the Marshall-Palmer distribution [eq (1)] gives the following rate of sublimation:

$$\mathrm{P4}=\frac{1}{\rho_a}\frac{\left(\frac{Q_v}{Q_{ts}}-1\right)(\rho_aQ_i)^{0.525}f_0^{-0.42}}{7\times10^5+\frac{0.41\times10^7}{e_{ts}}} \tag{22}$$

where Q_v is the mixing ratio of water vapor, and Q_{ts} and e_{ts} are the saturation mixing ratio of water vapor and saturation vapor pressure (measured in mb) over a plane ice surface, respectively.

MELTING PROCESS

Ice crystals begin to melt when falling across the 0°C surface. With the Marshall-Palmer distribution, the rate of melting per unit time, P5, is given by (Mason, 1956):

$$\mathrm{P5}=2.27\times10^{-6}C(T-273)(\rho_aQ_i)^{0.525}\rho_a^{-1}f_0^{-0.42} \tag{23}$$

where C represents the ventilation coefficient given by

$$C=1.6+0.57\times10^{-3}(V_i)^{1.5}f_0^{-1}. \tag{24}$$

It is assumed that all melted water belongs to the category of raindrops and the remaining ice crystals still follow the Marshall-Palmer distribution law, continuing to fall with the velocity V_i.

EVAPORATION OF CLOUD DROPLETS

The equation for evaporation of cloud droplets is similar

to the equation for sublimation except for the terms of latent heat of sublimation and vapor pressure.[4]

EVAPORATION OF RAINDROPS

Evaporation of raindrops, P7, is also expressed by an equation similar to that for sublimation. The ventilation coefficient C is included in this case. It is assumed that the distribution of raindrops still follows the Marshall-Palmer distribution even in the process of evaporation. The equation is

$$\mathrm{P7}=-\frac{1}{\rho_a}\frac{\left(\frac{Q_v}{Q_{vs}}-1\right)C(\rho_a Q_r)^{0.525}}{5.4\times10^5+\frac{0.41\times10^7}{e_{ws}}} \tag{25}$$

where Q_{vs} is the saturation mixing ratio of water vapor, e_{ws} is the saturation vapor pressure over a plane water surface measured in mb and the ventilation coefficient was obtained by inserting the typical velocity of raindrops.

With the typical values of $Q_r=10^{-3}$gm/gm, $e_{ws}=10$ mb, and $V_w=5$ m/s, this equation gives 5.8×10^{-4} (Q_v-Q_{vs}) gm·gm^{-1}·s^{-1} as the rate of evaporation of raindrops. It is interesting to note that Kessler (1969) proposed a simpler equation which gives 5.4×10^{-4} (Q_v-Q_{vs}) gm·gm^{-1}·s^{-1} for a raindrop content of 10^{-3} gm·cm^{-3}.

EVAPORATION OF ICE CRYSTALS

The equation for evaporation of ice crystals, P8, is similar to that for raindrops except for different terms of latent heat of sublimation and vapor pressure. The equation in the case of the Marshall-Palmer distribution is

$$\mathrm{P8}=-\frac{1}{\rho_a}\frac{\left(\frac{Q_v}{Q_{is}}-1\right)C(\rho_a Q_i)^{0.525}f_0^{-0.42}}{7\times10^5+\frac{0.41\times10^7}{e_{is}}}. \tag{26}$$

EVAPORATION OF MELTING ICE CRYSTALS

The evaporation of melting ice crystals, P9, is expressed by the equation for the ice crystals except that the ice surface is wet. When the Marshall-Palmer distribution is used,

$$\mathrm{P9}=-\frac{1}{\rho_a}\frac{\left(\frac{Q_v}{Q_{vs}}-1\right)C(\rho_a Q_i)^{0.525}f_0^{-0.42}}{5.4\times10^5+\frac{0.41\times10^7}{e_{ws}}}. \tag{27}$$

3. FORMULATION OF THE PROBLEM

In this work, the cloud is modeled as a circular air column with a time-independent radius in an environment at rest. All equations will be formulated in one-dimensional space along the lines taken by Asai and Kasahara (1967) as far as the dynamic terms are concerned. The effect of compensating downward motions in the environment is not considered, however.

Within the framework of one-dimensional treatment, there is no way of determining the pressure distribution associated with the air motion. It is therefore assumed that the pressure adjusts instantaneously at any level to take the same value as that of the environment which is in hydrostatic equilibrium. Using the cylindrical coordinates (r, λ, z) where r, λ, and z denote the radial, tangential, and height coordinates, respectively, the equation for the vertical component of velocity may be written as

$$\rho_{a0}\frac{\partial w}{\partial t}+\frac{1}{r}\frac{\partial}{\partial r}(\rho_{a0}ruw)+\frac{1}{r}\frac{\partial}{\partial\lambda}(\rho_{a0}vw)+\frac{\partial}{\partial z}(\rho_{a0}ww)=\rho_{a0}g\left(\frac{T_v-T_{v0}}{T_{v0}}\right) \tag{28}$$

where u, v, and w are the radial (positive outward), tangential, and vertical (positive upward) components of the velocity, T_v is the virtual temperature and g the acceleration of gravity. The subscript zero denotes the quantities in the environment.

In deriving eq (28), the equation of mass continuity was used in the following form:

$$\frac{1}{r}\frac{\partial}{\partial r}(\rho_{a0}ru)+\frac{1}{r}\frac{\partial}{\partial\lambda}(\rho_{a0}v)+\frac{\partial}{\partial z}(\rho_{a0}w)=0. \tag{29}$$

The virtual temperature is related to the temperature, T, by the equation:

$$T_v=T(1+0.608\ Q_v). \tag{30}$$

The drag force provided by the weight of liquid and solid water will be added to eq (28) later.

We integrate eq (28) and (29) over the cross section of the cloud column which has a radius a and then divide the resulting equations by $\rho_{a0}\pi a^2$ to derive the following equations:

$$\frac{\partial\overline{w}}{\partial t}+\frac{2}{a}(\tilde{u}_a\tilde{w}_a+\widetilde{u_a''w_a''})+\frac{1}{\rho_{a0}}\frac{\partial}{\partial z}[\rho_{a0}(\overline{u}\,\overline{w}+\overline{u'w'})]=g\frac{\overline{T}_v-T_{v0}}{T_{v0}} \tag{31}$$

and

$$\frac{2}{a}\tilde{u}_a+\frac{1}{\rho_{a0}}\frac{\partial}{\partial z}(\rho_{a0}\overline{w})=0. \tag{32}$$

Here, we used the following notations for any variable A:

$$\overline{A}=\frac{1}{\pi a^2}\int_0^{2\pi}\int_0^a Ardrd\lambda,$$

$$\tilde{A}_a=\frac{1}{2\pi}\int_0^{2\pi}Ad\lambda \quad \text{at } r=a, \tag{33}$$

and

$$A'=A-\overline{A},\quad A_a''=A-\tilde{A}_a$$

where the subscript a denotes the quantities at $r=a$.

The term containing $\widetilde{u_a''w_a''}$ represents the lateral eddy exchange of momentum between the cloud and the environment at rest and is very important from the viewpoint

[4] A computation was repeated where, instead of computing P6, cloud droplets were assumed to evaporate instantaneously as long as the air was not saturated with water vapor. It turned out that this change produced no significant difference in the resulting velocity field.

of entrainment. We will retain this term, therefore, ignoring, however, the term containing $\overline{w'w'}$ (see section 8 for further discussion). We further assume

$$\widetilde{u_a''w_a''}=\frac{\nu}{a}\overline{w} \tag{34}$$

where ν denotes the kinematic eddy exchange coefficient. From dimensional reasoning, ν may be expressed as

$$\nu=\alpha^2 a|\overline{w}| \tag{35}$$

where α^2 is a proportionality constant (see section 4 for the value of α^2 used in the model).

With the aid of eq (34) and (35), adding now the drag force and omitting hereafter the bar symbol, eq (31) is written as

$$\frac{\partial w}{\partial t}=-w\frac{\partial w}{\partial z}-\frac{2\alpha^2}{a}w|w|+\frac{2}{a}(w-\tilde{w}_a)\tilde{u}_a +g\frac{T_v-T_{v0}}{T_{v0}}-g(Q_c+Q_r+Q_i). \tag{36}$$

In this equation, $\tilde{u}_a$ will be determined by eq (32) with the boundary condition that $w=0$ at $z=0$. The quantity $\tilde{w}_a$ is still unspecified. We assume for any variable, A, that

$$\tilde{A}_a=A_0, \quad \text{if } \tilde{u}_a<0, \tag{37}$$

and

$$\tilde{A}_a=A, \quad \text{if } \tilde{u}_a>0.$$

The first term in the right-hand side of eq (36) represents the vertical advection, the second term the lateral eddy exchange, the third term the dynamic entrainment that is required to satisfy the mass continuity between the cloud and the environment, the fourth term the buoyancy, and the last term the drag force that is assumed to be provided by the weight of cloud droplets, raindrops, and ice crystals.

It is to be noted that, in the other one-dimensional cloud models (Simpson et al. 1965, Simpson and Wiggert 1969, 1971), the dynamic interaction between cloud and environment is represented in terms of entrainment that is inversely proportional to the element radius (see also Simpson 1971). In contrast, our model represents entrainment in two terms: the lateral mixing at the wall of the rising cloud and the systematic inflow to or outflow from the cloud through the side wall. In this respect, the present model may be regarded as a "one and a half" dimensional model. Both terms are inversely proportional to the element size.

Similarly, the thermodynamic equation is written as

$$\frac{\partial T}{\partial t}=-w\left(\frac{\partial T}{\partial z}+\Gamma_d\right)+\frac{2\alpha^2}{a}|w|(T_0-T)+\frac{2}{a}\tilde{u}_a(T-\tilde{T}_a) +\left[\frac{L_s}{c_p}(\mathrm{P1}-\mathrm{P6}-\mathrm{P7}-\mathrm{P9}) +\frac{L_s}{c_p}(\mathrm{P4}-\mathrm{P8})+\frac{L_f}{c_p}(\mathrm{P3}-\mathrm{P5})\right] \tag{38}$$

where c_p is the specific heat of air, Γ_d is the dry adiabatic lapse rate, and L_v, L_s, and L_f are the latent heat of evaporation (600 cal/gm), latent heat of sublimation (680 cal/gm), and latent heat of fusion (80 cal/gm), respectively.

The equations of continuity for water vapor, cloud droplets, raindrops, and ice crystals, respectively, are

$$\frac{\partial Q_v}{\partial t}=-w\frac{\partial Q_v}{\partial z}+\frac{2\alpha^2}{a}|w|(Q_{v0}-Q_v)+\frac{2}{a}\tilde{u}_a(Q_v-\tilde{Q}_{va}) -\mathrm{P1}+\mathrm{P6}+\mathrm{P7}+\mathrm{P8}-\mathrm{P4}+\mathrm{P9}, \tag{39}$$

$$\frac{\partial Q_c}{\partial t}=-w\frac{\partial Q_c}{\partial z}+\frac{2\alpha^2}{a}|w|(Q_{c0}-Q_c) +\frac{2}{a}\tilde{u}_a(Q_c-\tilde{Q}_{ca})+\mathrm{P1}-\mathrm{P2}-\mathrm{P6}, \tag{40}$$

$$\frac{\partial Q_r}{\partial t}=-(w-V_w)\frac{\partial Q_r}{\partial z}+\frac{Q_r}{\rho_{a0}}\frac{\partial(\rho_{a0}V_w)}{\partial z}+\frac{2\alpha^2}{a}|w|(Q_{r0}-Q_r) +\frac{2}{a}\tilde{u}_a(Q_r-\tilde{Q}_{ra})+\mathrm{P2}-\mathrm{P3}-\mathrm{P7}+\mathrm{P5}, \tag{41}$$

and

$$\frac{\partial Q_i}{\partial t}=-(w-V_i)\frac{\partial Q_i}{\partial z}+\frac{Q_i}{\rho_{a0}}\frac{\partial(\rho_{a0}V_i)}{\partial z}+\frac{2\alpha^2}{a}|w|(Q_{i0}-Q_i) +\frac{2}{a}\tilde{u}_a(Q_i-\tilde{Q}_{ia})+\mathrm{P3}+\mathrm{P4}-\mathrm{P5}-\mathrm{P8}-\mathrm{P9}. \tag{42}$$

If we define the total water content, Q, by $Q=Q_v+Q_c+Q_r+Q_i$, the combination of the above four equations and the mass continuity equation [eq (32)] gives the following conservation equation for Q:

$$\rho_{a0}\frac{\partial Q}{\partial t}=-\frac{\partial(\rho_{a0}Qw)}{\partial z}+\frac{\partial}{\partial z}(\rho_{a0}V_wQ_r+\rho_{a0}V_iQ_i) -\frac{2}{a}\rho_{a0}\tilde{u}_a\tilde{Q}_a+\frac{2\alpha^2}{a}\rho_{a0}|w|(Q_0-Q). \tag{43}$$

4. NUMERICAL PROCEDURE

The equations derived in the previous section were integrated numerically as an initial value problem by a finite-difference method. The method we used is the "forward-upstream" scheme which uses forward time-extrapolation for the local changes with time, and upstream space-differencing in the advection terms of the equations. All spatial derivatives, other than those in the advection terms of the equations, are replaced by centered differences. The space increment (Δz) was 250 m and the time increment (Δt) was 5 s.[5]

We tested two different schemes for computing the vertical advection terms: (1) w was averaged over three gridpoints, one below and one above the gridpoint being considered; and (2) w was averaged over two gridpoints, one below the point if $w\geq 0$ or one above if $w<0$. The results indicate that the first scheme gives a maximum vertical velocity 20 percent smaller than that obtained by the second scheme. As demonstrated by Molenkamp (1968), a

[5] Test runs were made using three different values for Δz : 100, 200, and 400 m. The maximum updrafts computed agree with each other within 10 percent errors.

strong dumping effect is implicit in the forward-upstream differencing scheme. Because it was desired to reduce this effect as much as possible, the second scheme was applied throughout this experiment.

The boundary conditions we used are those where the vertical velocity vanishes both at the surface and at the top of the atmosphere, which was assumed to be 15 km high; Q_c, Q_r, and Q_i are assumed to be zero and T and Q_v are fixed at both boundaries.

The environmental atmosphere used in most cases of this series of calculations has a temperature lapse rate (denoted by Γ_0) of 6.3°C/km up to 10 km and is isothermal above that level. The temperature at the surface is 25°C. The relative humidity at the surface in this hypothetical atmosphere is 100 percent and decreases upward at a rate 5 percent per km. Q_c, Q_r, and Q_i are assumed to be zero in the environmental atmosphere.

Motion in this environmental atmosphere was initiated by introducing a small updraft that has the form

$$w_{t=0}=\Delta w\left(\frac{z}{z_0}\right)\left(2-\frac{z}{z_0}\right) \tag{44}$$

in the layer below 2 km where Δw = 1 m/s and z_0 = 1 km. The radius of the cumulus air column was assumed to be 3 km.

There are some difficulties in choosing a proper value of the lateral mixing parameter (α^2). In a classical model for a one-dimensional steady-state jet or buoyant rising plume, the mass continuity equation is expressed in our notation as

$$\frac{d}{dz}(a^2\rho_a w)=2a\gamma\rho_a w \tag{45}$$

with a proportionality constant γ (cf., Squires and Turner 1962). If we define the quantity $M=a^2\rho_a w$ proportional to the mass flux at height z, eq (45) may be rewritten approximately as

$$\frac{1}{M}\frac{dM}{dz}\approx\frac{2\gamma}{a}. \tag{46}$$

The momentum equation for a jet in an incompressible fluid is written as

$$\frac{d}{dz}(Mw)=0. \tag{47}$$

With eq (47), eq (46) is transformed to

$$\frac{dw}{dz}\approx-\frac{2\gamma}{a}w. \tag{48}$$

After a careful survey of the literature, Morton (1959) concluded that the most accurate value of γ could be obtained from experiments on jets in air and adopted the value of $\gamma=0.116$. Later, Ricou and Spalding (1961) arrived at a value equivalent to $\gamma=0.080$. Squires and Turner (1962) used $\gamma=0.10$ in their model for cumulonimbus updrafts and Simpson and Wiggert (1969) used a value equivalent to $\gamma=0.09$ in their model for precipitating cumulus towers.

As mentioned before, the dynamic interaction between cloud and environment in our model is represented by two terms: lateral eddy exchange and dynamic entrainment. If we suppress in eq (36) the terms of time derivative, dynamic entrainment, buoyancy, and drag forces, the equation may be written approximately as

$$\frac{\partial w}{\partial z}\approx-\frac{\alpha^2}{a}w. \tag{49}$$

In other words, the lateral eddy mixing in our model has the same form as that for entrainment in other one-dimensional cloud models.

Asai and Kasahara (1967) used $\alpha^2=0.1$ and $\alpha^2=1.0$ in their cumulus modeling study. At the preparatory stage of our study, two runs were made with identical initial and environmental conditions but with different values for α^2. The maximum updraft obtained was 14.1 m/s with $\alpha^2=0.1$ whereas it was only 4.8 m/s with $\alpha^2=1.0$. We prescribed the value of $\alpha^2=0.1$ rather arbitrarily in this series of calculations. A more accurate value should be determined by applying the model to real cloud data.

The actual calculations proceed in the following manner:

1. $\tilde{u}_a$ is calculated from the known w using eq (32).
2. V_w and V_i are calculated using eq (14) and (18).
3. The new value of w and dummy values T^*, Q_v^*, Q_c^*, Q_r^*, and Q_i^* at the next time step are calculated taking into account only the dynamical terms in the above prognostic equations.
4. Saturation mixing ratios corresponding to T^* are derived, where saturation mixing ratios over water (Q_{ws}) and over ice (Q_{is}) as functions of temperature T are given by

$$Q_{ws}=3.8p^{-1}10\,\frac{7.5(T-273)}{T-36} \tag{50}$$

and

$$Q_{is}=3.8p^{-1}10\,\frac{9.5(T-273)}{T-8} \tag{51}$$

where p is the environmental atmospheric pressure.

5. The quantity P1 is calculated as $(Q_v^*-Q_{vs})/\Delta t$. The quantities P2, . . . , P9 are calculated using the formulas given in section 2. These calculations include many judgments such as $T^*\gtreqless 273$, $Q_v^*\gtreqless Q_{vs}(T^*)$, $Q_r^*\gtreqless 0$, and $Q_i^*\gtreqless 0$. Sometimes two or three cloud physical processes take place at the same time. For instance, in subsaturated air, evaporation of raindrops, cloud droplets, and ice crystals may occur during the same period. In such a case, we assume that cloud droplets evaporate first. If air is still unsaturated, we let raindrops and ice crystals evaporate. The conditions that the total amount of evaporation cannot exceed the saturation water vapor must hold at all times. The lengthy flow chart is not reproduced here.
6. The values of T, Q_v, Q_c, Q_r, and Q_i at the next time step are computed with the inclusion of P1, . . . , P9. This completes one cycle of time integration.

5. RESULTS AND DISCUSSIONS

A SOLUTION WITHOUT DRAG FORCE AND RAIN FORMATION

The first solution to be presented is calculated with assumptions similar to those applied by Asai and Kasahara (1967); all condensed water vapor forms liquid water that remains in the cloud without falling out of the cloud and the drag force provided by the weight of liquid water is ignored. Comparison of the solutions with those in the next subsection will illustrate the importance of these ignored processes and the drag force in the life cycle of a thunderstorm cell.

Figures 2A–2C show the time-height cross-sections of vertical velocity, temperature difference between inside the cloud and the environment, and total liquid content. The primary feature of the cross-sections is that the cloud reaches a steady state after approximately 40 min. For example, figure 2A shows that the vertical velocity increases slowly during the first 20 min, develops rapidly, and then becomes stationary after 40 min with the maximum updraft of 27 m/s. A similar steady-state solution was obtained by Asai and Kasahara (1967) and Weinstein (1970).

The maximum temperature difference observed in figure 2B is 3.2°C. Strongly negative excess temperature appears at the height of 11 km, apparently caused by the forced upward motion in the upper isothermal layer. The liquid water content increases and the region having maximum liquid water content increases its height with time before approximately 40 min (fig. 2C). The maximum liquid water content in the steady state is 8 gm/kg and it appears at the 9-km level.

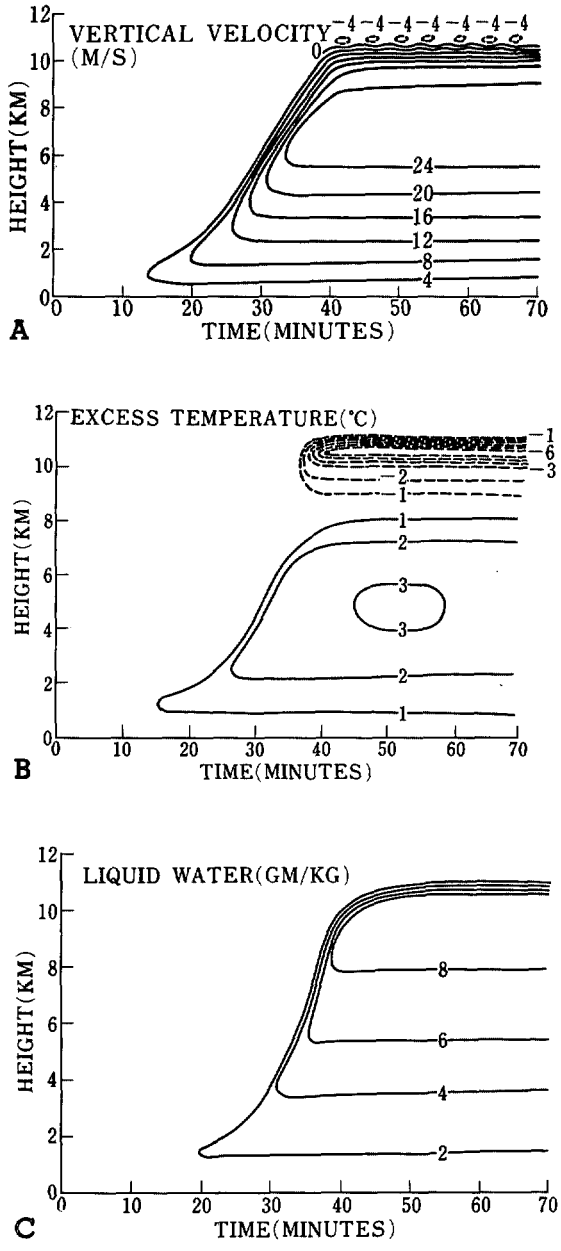

FIGURE 2.—Time-height cross-sections of (A) vertical velocity, (B) excess temperature, and (C) liquid water content for a cloud without microphysical processes.

A TYPICAL SOLUTION WITH CLOUD MICROPHYSICAL PROCESSES

When all microphysical processes described in section 2 and the drag force are incorporated into the model, the character of the solution is completely different from the previous one.

Figure 3 shows the time-height cross-sections of vertical velocity, temperature difference, total hydrometeor (liquid and solid water) content, cloud droplet content, raindrop content, and ice crystal content. In this case, Co is 0.005, f_0 is 0.75, G is 0.005 and the Marshall-Palmer distribution is used for both raindrops and ice crystals.

We observe in figure 3A that the updraft increases after 20 min and the height of the region of maximum updraft increases with time in the same way as the case without cloud physical processes. A downdraft, however, starts developing first in the lower part of this cloud at 40 min and spreads to the higher altitude. At approximately 60 min, the downdraft replaces the updraft throughout the domain. In particular, a strong downdraft appears at the melting zone. After the strong downdraft reaches the ground, the downdraft decreases and soon dies. The maximum updraft is 17 m/s and the maximum downdraft is 5 m/s.

The excess temperature shown in figure 3B increases with time at first in a way similar to that in the case without microphysical processes. After 40 min, however, it begins to decrease in value. At 55 min a negative temperature difference is observed near the melting level where the strong downdraft developed. The maximum excess temperature is 2.8°C and is observed at 5 km while the maximum updraft is found at the 7-km level.

The total liquid and solid water content ($Q_c+Q_r+Q_i$) reaches its maximum value of 8 gm/kg at approximately 50 min and at a height of 8 km (fig. 3C).

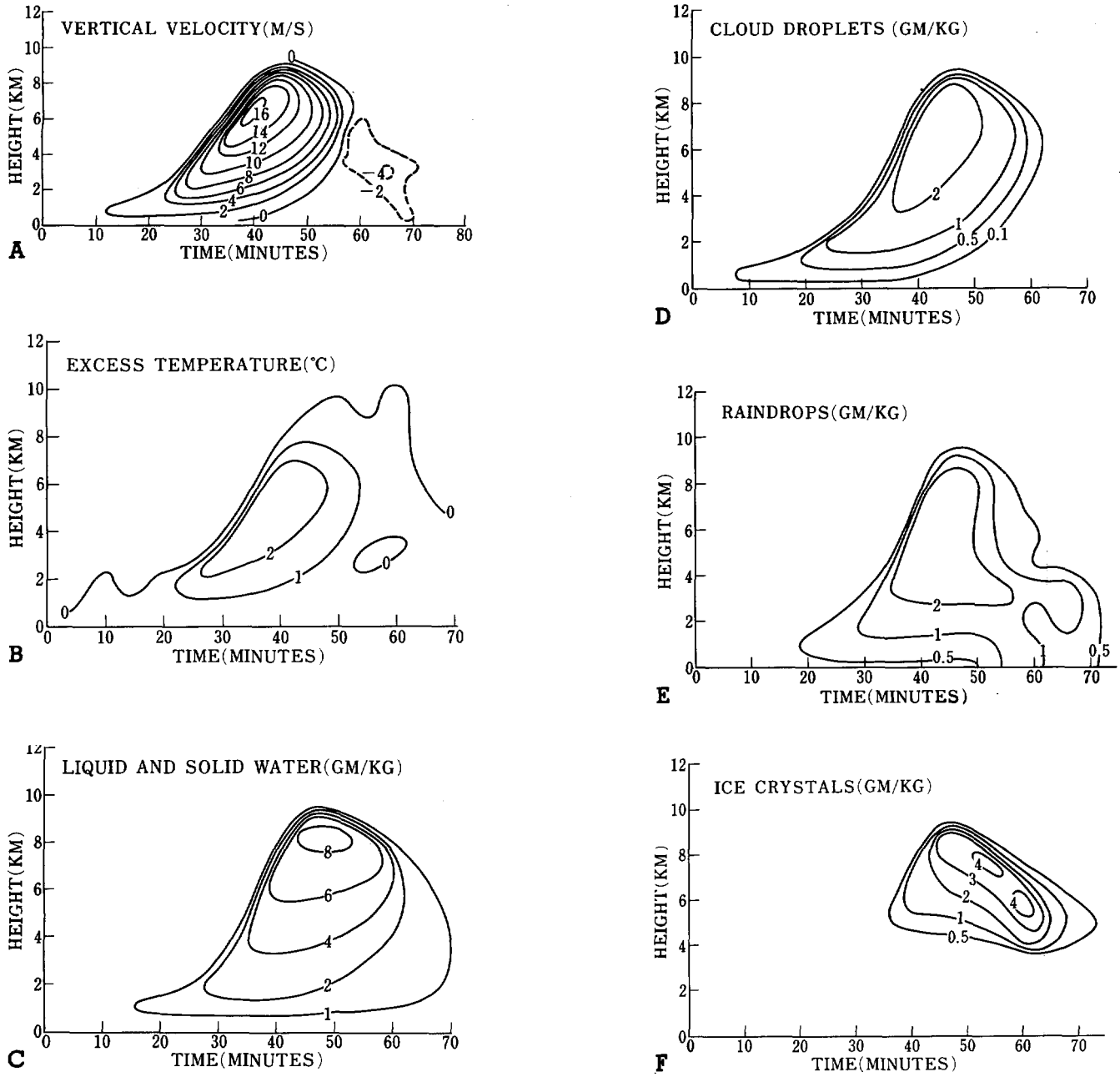

FIGURE 3.—Time-height cross-sections of (A) vertical velocity, (B) excess temperature, (C) liquid and solid water content, (D) content of cloud droplets, (E) content of raindrops, and (F) content of ice crystals for a cloud with microphysical processes; $\Gamma_0 = -6.3$°C/km, $Co = 0.005$.

Figures 3D–3F present time-height profiles for the hydrometeors. The cloud droplet concentration (fig. 3D) has its maximum value at approximately 6 km and its magnitude is 3 gm/kg. After 65 min, the liquid water content of cloud droplets becomes less than 0.1 gm/kg and the cloud disappears. The raindrop content (fig. 3E) reaches its maximum also at approximately 45 min with the value of 2.8 gm/kg. After 50 min, the region of this maximum raindrop content decreases in both height and magnitude with the fallout of raindrops. However, a region of relatively high raindrop content appears at approximately 65 min in the region just below the melting layer. This large liquid water content may be accounted for by melting of ice crystals that, falling from the higher levels, reach this level at approximately 60 min (fig. 3F).

The development and structure of thunderstorms in the United States has been investigated extensively by Byers and Braham (1949), who divided the life cycle of a thunderstorm into three stages: developing stage, mature stage, and decaying stage. In the developing stage, there is a general updraft throughout the cloud and the towers grow upward at an appreciable rate. Although no precipitation may be falling out of the cloud, hydrometeors are present inside the cloud. The mature stage is taken to begin when rain first falls out of the base of the cloud. The regions of updraft and downdraft exist side by side. As the down-

draft spreads horizontally so that it occupies a major portion of the cloud, the dissipation stage sets in. There is then no appreciable source of water vapor to maintain condensation, and the cloud feeds mainly on the water already accumulated. The typical duration times for each stage are roughly 10–15 min, 15–30 min, and 30 min, respectively.

These three stages are well simulated in our numerical cloud model. For the particular initial conditions we applied, there is another stage that we may call the "nursing stage," occurring before the developing stage. In this nursing stage, the updraft remains weak and the cloud is not ready to make a rapid development. The duration times for these four stages are calculated respectively to be 20, 20, 15, and 20 min.

The motions we are dealing with in this article are buoyancy-generated motions and therefore it is important to examine heat sources and sinks inside the cloud. Figure 4 shows the contributions of various microphysical processes to the rate of change in temperature with time during the life cycle of a cell. This figure also illustrates the manner in which various water substances keep their balance.

As expected, release of latent heat by condensation of water vapor (P1) plays a dominate role in the change of temperature during the development and mature stages (fig. 4A). The maximum temperature change rate is approximately 0.15°C/s. This large amount of heating is, of course, compensated mostly by cooling due to volume expansion of air parcel. It is also interesting to point out that the vertical distribution of P1 has two maxima in the developing and mature stages. The rate of condensation of water vapor may be controlled by two factors—vertical velocity and the amount of water vapor. The latter is almost always decreasing in magnitude with altitude whereas the height of the maximum updraft increases with time. These two factors may account for the presence of two maxima of P1 after 25 min.

Evaporation of cloud droplets (P6) makes a significant contribution to the temperature change at the top of the cloud during the development stage (fig. 4B); the maximum rate of change in temperature due to this process is approximately 25 percent of that due to condensation. Evaporation of raindrops (P7) contributes only in the decaying stage in the lower portion of the cloud (fig. 4B), the maximum rate being 0.013°C/s; that is, one order of magnitude smaller than that of condensation. The contributions of evaporation of melting ice (P9) and evaporation of ice crystals (P8) are approximately of the same order of magnitude as that of evaporation of raindrops (P7) but effective in more limited regions of the cloud and over a very limited time (figs. 4A and 4B). The release of latent heat due to glaciation (P3) contributes approximately 0.025°C/s at its maximum value whereas that due to sublimation of water vapor to ice crystals (P4) makes only a negligibly small contribution (fig. 4D). On the other hand, the contribution of

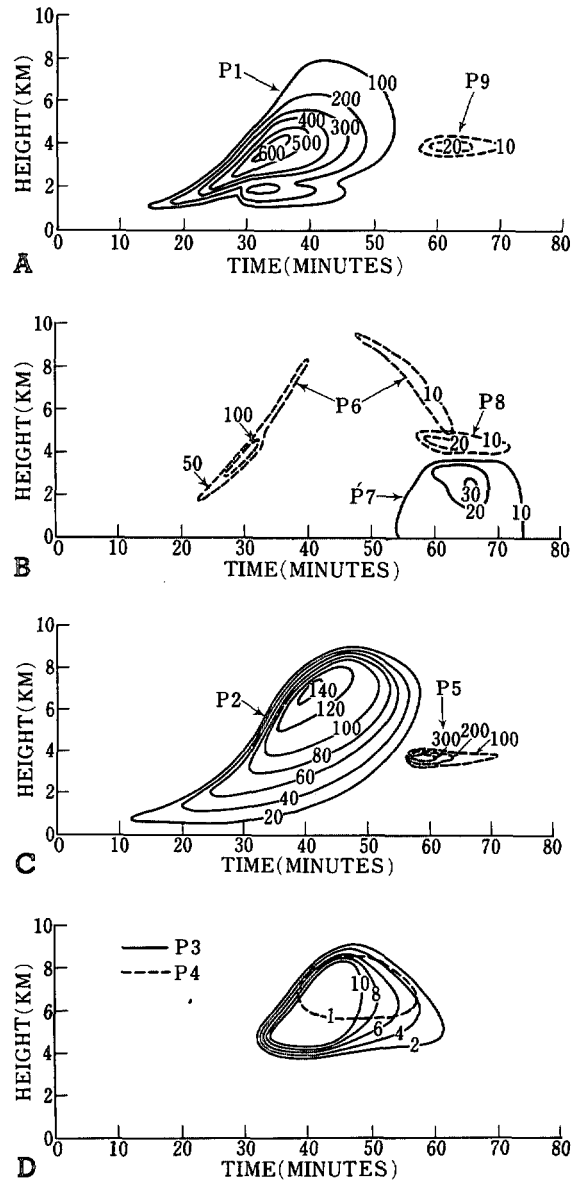

FIGURE 4.—Time-height cross-sections of the rates of (A) condensation of water vapor into cloud droplets (P1) and evaporation of melting ice crystals (P9); (B) evaporation of cloud droplets (P6), raindrops (P7), and ice crystals (P8); (C) conversion of cloud droplets into raindrops (P2) and melting of ice crystals (P5); and (D) glaciation (P3) and growth of ice crystals by sublimation (P4) in units of 10^{-7} s^{-1}.

melting of ice crystals (P5) is approximately 0.01°C/s at its highest and its contribution is limited only in the decaying stage and in a thin layer below the freezing level (fig. 4C).

Figure 5 shows the change of precipitation intensity with time as observed at the ground surface. The precipitation intensity reaches its first maximum with the value of approximately 36 mm/hr after 60 min and then decreases with time but reaches a second maximum after 70 min. From figure 3, it is apparent that this second maximum of precipitation is caused by the ice crystals;

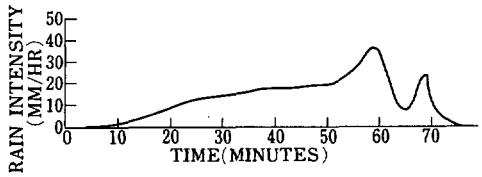

FIGURE 5.—Changes with time of precipitation intensity at the ground surface; $\Gamma_0 = -6.3$°C/km, $Co = 0.005$.

they fall from the upper portion of the cloud with smaller terminal velocity than that of raindrops and are transformed into raindrops when they fall through the freezing levels. The total amount of precipitation by this hypothetical thunderstorm cell during its entire life cycle is calculated as 17 mm·cm^{-2}.

Comparison of the present result with Weinstein's (1970) result indicates that the strong downdraft which continues to be present in the lower half of the atmosphere in Weinstein's model is not seen in the present result. The oscillatory feature of motion that is seen in the decaying stage in his result, and seen also in Srivastava's (1967) result, is not present here.

COMPARISON WITH OBSERVATIONS

As stated in section 1, it is not the intention of this article to make a quantitative comparison between the numerical result and the observed data because so many simplifications are introduced into the model and hypothetical vertical distributions of temperature and humidity are applied to the ambient atmosphere. Nevertheless, it may be instructive to make some comparisons.

We have already mentioned that our model simulates three stages of the life cycle of a thunderstorm as proposed by Byers and Braham (1949) and that the duration times for each stage as predicted by the model are rather close to those observed. At the developing stage, the maximum updraft was observed at the top of the cloud in the thunderstorm project. The profile of updraft in our study is very similar to that of the observation, and the maximum updraft is present near the top of the cloud. The magnitude of maximum updraft was 17 m/s in the observation and this value is the same as that in our study (fig. 3A). The excess temperature was 3°C in the thunderstorm project, whereas the maximum excess temperature of 2.8°C is calculated (fig. 3B). A strong downdraft was observed at the mature stage in both the observations and this calculation. However, the magnitude of the downdraft was 13 m/s in the observation while this model gives a downdraft of only 5 m/s. The maximum temperature difference from the ambient atmosphere was −3°C in the thunderstorm project while it is only −0.3°C in the calculation. Undoubtedly, this disagreement is due in part to the high humidity we applied in the lower layer of the ambient atmosphere so that the effect of strong evaporation from falling raindrops that would take place below the cloud base is not simulated.

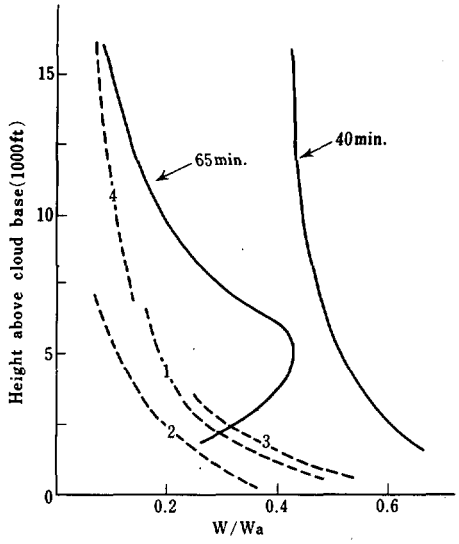

FIGURE 6.—Vertical distributions of liquid water content as calculated (solid lines) at $t = 40$ min and $t = 65$ min. Dashed lines show the observed results: curve 1, Warner (1955); curve 2, Squires (1958); curve 3, Ackerman (1959); and curve 4, Ackerman (1963).

Weickmann (1969) observed the temperature difference between the inside and outside of the cloud. Excess temperature up to 2.5°C was observed at the height of 2.6 km. Battan and Theiss (1966) observed the vertical motion in a thunderstorm by Doppler radar and found strong updraft and high echo intensity in the upper part of the cloud with the maximum updraft exceeding 19 m/s. These results are not inconsistent with our results in the developing stage.

The liquid water content in convective clouds has been observed in hurricanes by Ackerman (1963) and in cumuliform clouds of less severe weather by Warner (1955), Squires (1958) and Ackerman (1959). Only a small fraction of Ackerman's measurements were larger than 3 gm·m^{-3}. However, on two flights, water contents of 9.5 gm·m^{-3} and greater were encountered in the wall clouds and amounts up to 8 gm·m^{-3} were measured in a convective band about 100 mi from the center of the storm. She expressed the water contents (W) as fractions of the theoretical adiabatic water content (Wa); that is, the amount of water realized in parcel ascent from cloud base to measurement altitude with no dilution or rainout.

Figure 6 shows the vertical variation of water contents (W/Wa) as calculated by our model together with observed results. We observe that the calculated results in the developing stage are much larger than the observed results. On the other hand, all of the observational results can be compared favorably with the calculated results at the dissipating stage, except in the lower part of the cloud where a large water content due to melting ice crystals is calculated. For the purpose of verifying the numerical results, water content measurements covering the entire life cycle of an isolated cumulus cloud are required. An

additional requirement is that measurements must cover not only cloud droplets but also raindrops. One improvement in the numerical modeling would be to repeat the calculation with more realistic environmental conditions.

6. CONVERSION TIME

The parameter *Co* represents the rate at which cloud droplets produced by condensation of water vapor are converted to raindrops. The results described in the previous section were obtained with $Co=0.005$. The background information pertinent to determining a proper value of *Co* may be summarized in the following.

From the results of Twomey (1966), Bartlett (1966), Warshaw (1967), and Berry (1967, 1968), Mason (1969) estimated that the time taken for a cloud droplet to grow from 40 μm to a drizzle drop of radius 100 μm is 4 min in a cloud with a water content of 1 gm·m^{-3}. The *Co* value of 0.005 corresponds to the conversion time of 3.5 min.

The time taken by the cloud droplet to grow to 40 μm depends upon the initial size distribution of cloud droplets. When the initial distribution contains droplets of radius up to 25 μm with an initial droplet concentration of 200 cm^{-3}, mean-volume radius 10 μm, relative dispersion $\sigma_r/\bar{r}=0.15$, and liquid water content of 1 gm·m^{-3}, 7 min is necessary. Bartlett (1966) showed, however, that when the initial size distribution contains droplets of 30 μm in radius, the time is 2 min. The time depends strongly upon the distribution of sea salt nuclei and condensation nuclei and is much longer in continental air. Warshaw (1967) introduced the sedimentation effect and the time taken for droplet growth from 25 μm to 50 μm in radius was then found to be 5 min. Kovetz and Olund (1969) calculated the drop growth assuming a constant updraft of 10 cm/s and a supersaturation of 0.1 percent and found that 100 m^{-3} liquid drops larger than 100 μm in radius develop in 400 s.

Because of the uncertainty involved in the selection of a proper value of *Co*, computations have been repeated with $Co=0.001$, 0.01, 0.05, and 0.2, other conditions being held unchanged. Some of the results are shown in figure 7. Evidently, when the *Co* factor is larger than 0.005, the cloud undergoes a life cycle; the larger the *Co* factor is, the shorter the life time becomes. When $Co=0.001$ (fig. 7A), the cloud starts developing after 20 min and then becomes stationary, similar to the case where no microphysical processes were incorporated (fig. 2). However, it should be pointed out that the drag force due to the weight of liquid water is ignored in the case shown in figure 2 whereas it is included in this case.

We may then ask why the cloud attains a steady state when cloud droplets are converted to raindrops at a small rate. The answer may be found in figure 8 which shows the height-time cross-section for liquid water with $Co=0.001$. The distribution of ice crystals is not shown on this figure. The maximum raindrop concentration value of 1.4 gm/kg is at a height of approximately 9.5 km. In

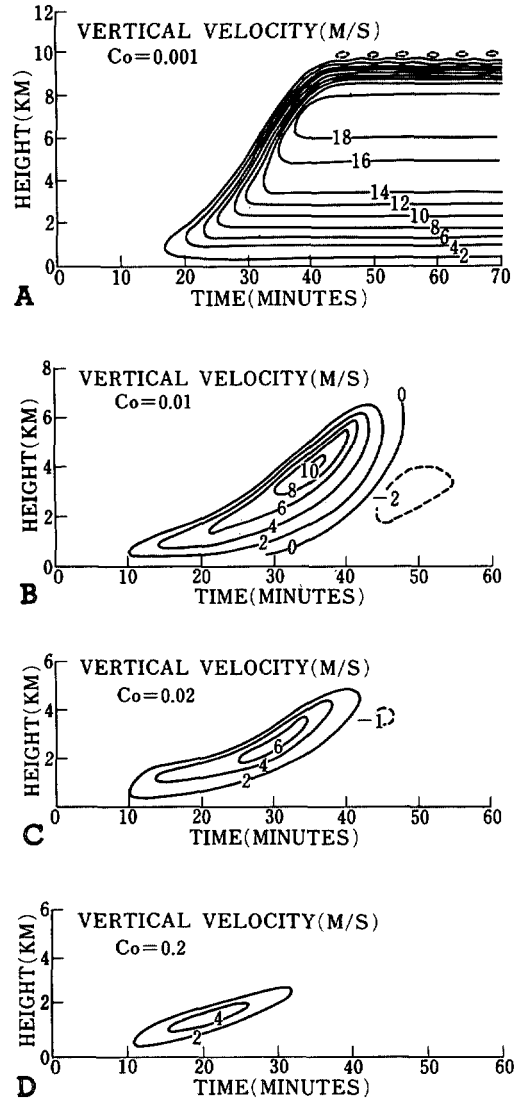

FIGURE 7.—Time-height cross-sections of vertical velocity for various values of the conversion parameter (*Co*); $\Gamma_0=-6.3$°C/km.

contrast to figure 3, we observe in figure 8 that (a) the amount of raindrops is extremely small while the amount of cloud droplets is very large with a maximum value of 6.3 gm/kg and (b) the amount of liquid and solid water is very small in the middle layer of the atmosphere.

In other words, cloud droplets produced by condensation of water vapor are carried by the updraft to the upper layer of the atmosphere without producing many raindrops. This makes liquid water content small (and consequently the drag force weak) in the middle portion of the cloud where the buoyancy force is acting. The large amount of liquid and solid water in the upper portion of the cloud may be easily suspended by the strong updraft which is present there.

When the *Co* parameter is large, raindrops are produced rapidly, and the large number of hydrometeors in the lower portion of the cloud tend to counteract the buoyancy force; this prevents further development of the cloud.

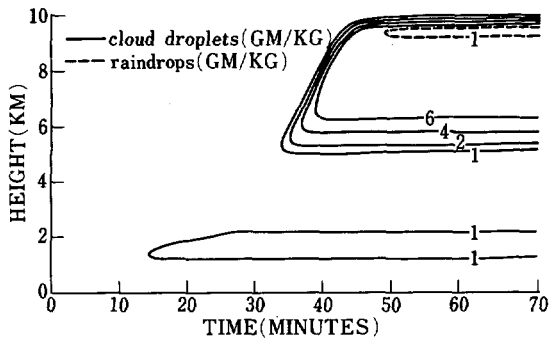

FIGURE 8.—Time-height cross-section of liquid water content; $Co=0.001$, $\Gamma_0=-6.3$°C/km.

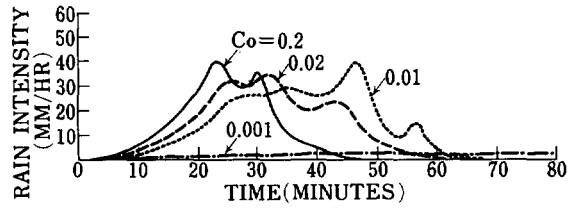

FIGURE 9.—Changes with time of precipitation intensities for various values of Co; $\Gamma_0=-6.3$°C/km.

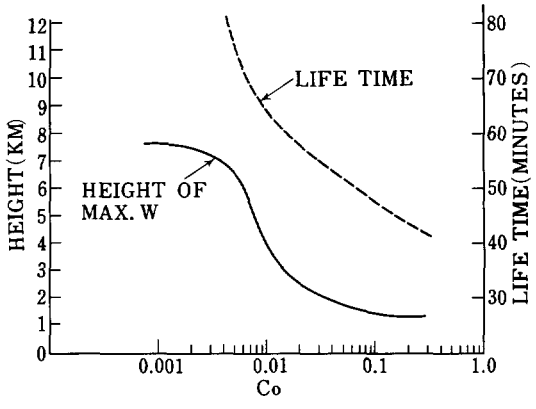

FIGURE 10.—Relation between Co and height at which vertical velocity is maximum and relation between Co and the lifetime of a cloud.

This is reflected in the change of precipitation intensity at the ground surface with time for various Co parameters (fig. 9). As Co becomes larger, rainfall starts earlier and ends earlier.

Figure 10 shows the relation between the Co factor and the height at which the vertical velocity reaches maximum values for an individual cloud and the relation between the Co factor and the lifetime of the cloud. By definition, the life of a cloud ends when the rate of precipitation at the ground surface becomes less than 1 mm/hr. We can see from figure 10 that the lifetime is 75 min for $Co=0.005$ while it is only 45 min when $Co=0.2$.

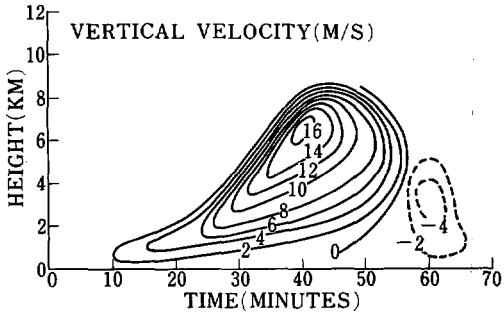

FIGURE 11.—Time-height cross-section of vertical velocity with exclusion of glaciation process; $\Gamma_0=-6.3$°C/km and $Co=0.005$.

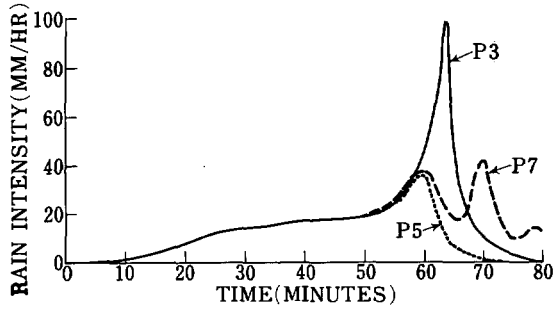

FIGURE 12.—Changes with time of precipitation intensities when one of the microphysical processes, as indicated in the figure, is excluded.

7. RELATIVE IMPORTANCE OF VARIOUS MICROPHYSICAL PROCESSES

To investigate the effects of various microphysical processes on the life cycle of a thunderstorm cell, we repeated the calculations excluding one of the P factors. The Co parameter is fixed at 0.005.

1. When the effect of evaporation of raindrops (P7) is excluded, the profile of the updraft does not change, but the downdraft changes; the strong downdraft near the melting level as observed in figure 3A does not appear and the maximum downdraft is reduced to 3 m/s. After 60 min, oscillatory behavior is observed.

2. When evaporation of cloud droplets (P6) is excluded, there is little change in the updraft region, though the time required to reach the maximum updraft is 5 min less and the value of the downdraft near the surface decreases.

3. The exclusion of evaporation of ice (P8) and evaporation of melting ice (P5) changes the profile of vertical velocity very little. The same is true for the exclusion of the sublimation term of ice crystals (P4).

4. The exclusion of the glaciation term (P3) makes the updraft smaller (fig. 11); the maximum updraft is 16 m/s instead of 17 m/s with this term. The downdraft pattern is considerably different from the previous case; the downdraft at the melting level disappears and instead a rather strong downdraft of 5.7 m/s appears 5 min earlier.

5. When melting of ice crystals (P5) is excluded, the downdraft at the melting level disappears and the strength of downdraft is much weaker (the maximum value is 3.8 m/s).

The effect of exclusion of various terms is also reflected in the change of precipitation intensity with time (fig. 12).

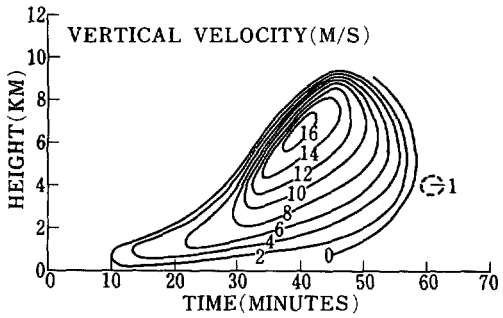

FIGURE 13.—Time-height cross-section of vertical velocity with Gunn-Marshall distribution for ice crystals; $\Gamma_0 = -6.3$°C/km and $Co = 0.005$.

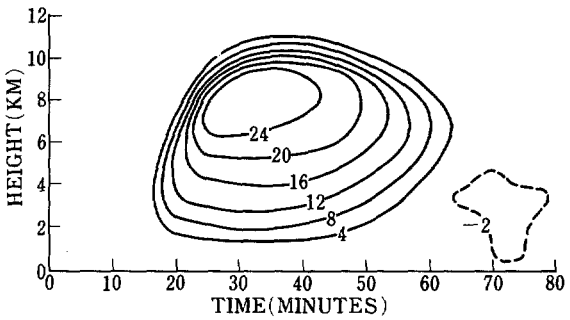

FIGURE 14.—Time-height cross-section of vertical velocity, $\Gamma_0 = -6.9$°C/km and $Co = 0.01$.

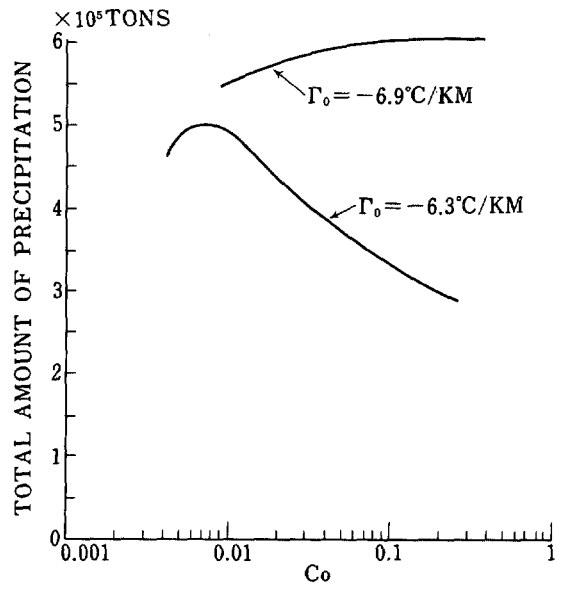

FIGURE 15.—The total amount of precipitation as a function of Co; $\Gamma_0 = -6.3$°C/km and -6.9°C/km.

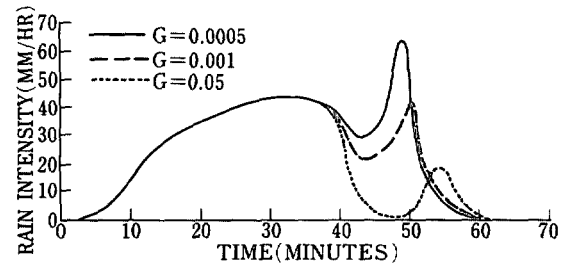

FIGURE 16.—Changes of precipitation intensity with time for various values of the glaciation factor, G; $\Gamma_0 = -6.9$°C/km and $Co = 0.2$.

Three cases where sublimation (P4), evaporation of ice crystals (P8), and evaporation of melting ice (P9) are excluded are not shown in this figure because there are only small differences from what is shown in figure 5. Elimination of the evaporation of raindrops (P7) results in the two peaks being observed about 3 min earlier than in the case including this term. Elimination of the raindrop evaporation terms (P7) results in a strong second peak. The second peak disappears when the melting term (P5) is eliminated.

The greatest change is obtained when the glaciation term (P3) is eliminated. A strong and sharp precipitation maximum is observed at 64 min.

For comparison, one case was computed with the Gunn-Marshall distribution for ice crystals (fig. 13) instead of the Marshall-Palmer distribution. The formulas for P4, P5, P8, and P9 with the Gunn-Marshall distribution are, of course, different from those given in section 2. The values of the parameters are the same as those in section 5. Comparing figure 13 with figure 3A, we observe that there is little change in the updraft pattern though the downdraft is much weaker. The second peak in the change of precipitation intensity with time does not appear in this case.

Finally, to investigate the sensitivity of the life cycle of a thunderstorm cell to the temperature lapse rate in the ambient atmosphere, we repeated the calculation using a lapse rate of 6.9° C/km instead of 6.3° C/km as in previous cases in the layer below 10 km. All other parameters remained unchanged. Figure 14 shows an example where $Co = 0.01$. Comparing this with figure 7B, we observe that this increase in temperature lapse rate enhances the development of the model cloud considerably.

Figure 15 shows the total amount of precipitation observed at the ground over the entire area of a cloud of 3-km radius for various values of the Co factor. It is interesting to note that there is an optimum value for Co corresponding to the largest precipitation amount in the case of $\Gamma_0 = -6.3$° C/km. This tendency is not observed for the case of $\Gamma_0 = -6.9$ °C/km.

Figure 16 shows the change of precipitation intensity with time for various values of the glaciation time, G, for $\Gamma_0 = -6.9$° C/km and $Co = 0.2$. The magnitude of the second peak decreases with increasing G.

8. CONCLUDING REMARKS

In this article, an attempt was made to simulate the life cycle of a thunderstorm cell. Extremely simple parameterized formulations were applied for conversion and glaciation processes. The promising result obtained here suggests the future extension of the present work along two different lines.

One immediate task is to refine this one and a half dimensional model in many aspects, applying it to real observational cases. Woodward (1959) showed from laboratory experiments that 60 percent of the mixing with outside air takes place at the front of the rising thermal, while Squires (1958) showed it to be plausible that the major part of entrainment into a real cloud occurs in this way. The present model does not include an explicit representation of the vertical mixing. The vertical mixing is implicit in the finite-differencing scheme. A proper value of the parameter of the lateral mixing (α^2) should also be determined by testing the present model against real cloud data.

There is also room for improvement in our parameterization of the glaciation process. The rate of glaciation in eq (16) is assumed to be a constant in our model. Existing observations (Langham and Mason 1958) may be used to assume that this rate is proportional to the degree of supercooling. Another unrealistic condition of our model is the assumption that all ice crystals are of precipitation size and none of cloud size. This is implied when the Marshall-Palmer or Gunn-Marshall spectra are used. In the study of the glaciating behavior of summertime cumulus clouds, Koenig (1963) observed that clouds having large liquid-water drops rapidly formed high concentrations of ice particles, and he particularly noted the rapidity with which the liquid-to-solid phase transition seemed to spread through a cloud volume. Our assumption is based mostly on his observations. Nevertheless, it would be a step toward realism to have small ice crystals of the size of Q_c and to have larger crystals growing by autoconversion, collection, and riming. Some work along this line have been done recently by Simpson and Wiggert (1969, 1971) and in a very sophisticated way by Cotton (1970).

More important, however, may be the proper parameterization of conversion from cloud droplets to raindrops as far as the dynamic behavior of cumulus clouds is concerned. The present investigation shows that the rate of conversion is the most important parameter in determining life cycle of a cloud cell. By using the parameterized formulation proposed by Kessler (1969), Weinstein (1970) also showed that changes in the threshold of cloud water produced significant changes in the rainfall characteristics. As mentioned in section 2, the problem of collection is one of the areas in cloud physics where there is no completely accepted explanation. Recently, Warner (1970) made a critical examination of existing steady-state one-dimensional cloud models. He indicated that such models cannot simultaneously predict values of liquid water content and cloud depth that are in agreement with observations. However, as pointed out by Simpson (1971), Warner's argument is based on a model which omits fallout of hydrometeors from the clouds.[6]

Another line of extension of the present work is to deal with the two- or three-dimensional model, aiming to describe the cloud in more complete detail. However, a two-dimensional treatment has its own problems except perhaps for clouds generated along a mountain ridge where the variations of meteorological variables along the mountain-ridge direction may be much smaller than those in the cross-mountain direction, so that the two-dimensional assumption may be applied with better accuracy than for an isolated cloud. The major problem would be the difference in microscale energy cascade processes between two- and three-dimensional motions (Kraichnan 1967, Leith 1968, Lilly 1969). In addition, the numerical result by Murray (1970) indicates that, because of the difference in geometries, the axisymmetric cloud model grows more vigorously than the rectilinear model and more realistically represents the relations between updraft and downdraft, the shape, and other characteristics. The three-dimensional convection then, may not be well simulated in two dimensions.

Nevertheless, a two-dimensional numerical simulation would be useful as a prelude to three-dimensional simulation to get some insight into the effect of the general flow on the maintenance of a cloud and into the interaction of cloud elements with each other and with their environment.

[6] Later in her unpublished paper, Simpson indicated that the Lagrangian-type cloud Model developed by Simpson and Wiggert (1969, 1971) gave correct cloud tops and water contents even with no precipitation fallout.

ACKNOWLEDGMENTS

The authors thank Marvin A. Geller for reading the manuscript and Betty Wolfe and Sandy Bryant for typing the manuscript. Thanks are also due Joanne Simpson and Edwin Kessler who read the first version of the manuscript and offered many useful comments. This work was initiated while one of the authors (T. T.) was Visiting Scientist at the Ocean Research Institute, the University of Tokyo, Japan, in June 1969.

The computations were done on the Control Data Corp. 6600 computer at the National Center for Atmospheric Research which is sponsored by the National Science Foundation. The work was supported by the Atmospheric Sciences Section, National Science Foundation, NSF Grant GA-020328.

REFERENCES

Ackerman, Bernice, "The Variability of the Water Contents of Tropical Cumuli," *Journal of Meteorology*, Vol. 16, No. 2, Apr. **1959**, pp. 191–198.

Ackerman, Bernice, "Some Observations of Water Contents in Hurricanes," *Journal of the Atmospheric Sciences*, Vol. 20, No. 4, July **1963**, pp. 288–298.

Arnason, Geirmundur, Brown, Philip S., and Chu, Roland T., "Numerical Simulation of the Macrophysical and Microphysical Processes of Moist Convection," *Proceedings of the WMO/IUGG Symposium on Numerical Weather Prediction, Tokyo, Japan, November 26–December 4, 1968, Technical Report* No. 67, Japan Meteorological Agency, Tokyo, Mar. **1969**, pp. I–11—I–21.

Arnason, Geirmundur, Greenfield, Richard S., and Newburg, Edward A., "A Numerical Experiment in Dry and Moist Convection Including the Rain Stage," *Journal of the Atmospheric Sciences*, Vol. 25, No. 3, May **1968**, pp. 404–415.

Asai, Tomio, "Numerical Experiment of Cumulus Convection Under the Pseudo-Adiabatic Process," *Papers in Meteorology and Geophysics*, Vol. 15, No. 1, Tokyo Meteorological Research Institute, Japan, Apr. **1964**, pp. 1–30.

Asai, Tomio, and Kasahara, Akira, "A Theoretical Study of the Compensating Downward Motions Associated With Cumulus Clouds," *Journal of the Atmospheric Sciences*, Vol. 24, No. 5, Sept. **1967**, pp. 487–496.

Bartlett, J. T., "The Growth of Cloud Droplets by Coalescence," *Quarterly Journal of the Royal Meteorological Society*, Vol. 92, No. 391, London, England, Jan. **1966**, pp. 93–104.

Battan, Louis J., and Theiss, John B., "Observations of Vertical Motions and Particle Size in a Thunderstorm," *Journal of the Atmospheric Sciences*, Vol. 23, No. 1, Jan. **1966**, pp. 78–87.

Beard, K. V., and Pruppacher, H. R., "A Wind Tunnel Investigation of Collection Kernels for Small Water Drops in Air," *Quarterly Journal of the Royal Meteorological Society*, Vol. 97, No. 412, London, England, Apr. **1971**, pp. 242–248.

Berry, Edwin X., "Cloud Droplet Growth by Collection," *Journal of the Atmospheric Sciences*, Vol. 24, No. 6, Nov. **1967**, pp. 688–701.

Berry, Edwin X., "Modification of the Warm Rain Process," *Proceedings of the First National Conference on Weather Modification, Albany, New York, April 28–May 1, 1968*, American Meteorological Society, Boston, Mass., **1968**, pp. 81–88.

Blanchard, Duncan C., "Raindrop Size-Distribution in Hawaiian Rains," *Journal of Meteorology*, Vol. 10, No. 6, Dec. **1953**, pp. 457–473.

Braham, Roscoe R., Jr., "What is the Role of Ice in Summer Rain-Showers?," *Journal of the Atmospheric Sciences*, Vol. 21, No. 6, Nov. **1964**, pp. 640–645.

Byers, Horace Robert, *Elements of Cloud Physics*, University of Chicago Press, Ill., **1965**, 191 pp. (see p. 162).

Byers, Horace Robert, and Braham, Roscoe R., Jr., *The Thunderstorm; Report of the Thunderstorm Project*, U.S. Government Printing Office, Washington, D.C., **1949**, 297 pp.

Caton, P. G. F., "A Study of Raindrop-Size Distributions in the Free Atmosphere," *Quarterly Journal of the Royal Meteorological Society*, Vol. 92, No. 391, London, England, Jan. **1966**, pp. 15–30.

Cotton, W. R., "A Numerical Simulation of Precipitation Development in Supercooled Cumuli," Ph. D. Dissertation, Pennsylvania State University, University Park, **1970**, 179 pp.

Das, Phanindramohan, "Role of Condensed Water in the Life Cycle of a Convective Cloud," *Journal of the Atmospheric Sciences*, Vol. 21, No. 4, July **1964**, pp. 404–418.

Davis, M. S., and Sartor, J. D., "Theoretical Collision Efficiencies for Small Cloud Droplets in Stokes Flow," *Nature*, Vol. 215, No. 5108, MacMillan Journals, Ltd., London, England, Sept. **1967**, pp. 1371–1372.

Durbin, W. G., "Droplet Sampling in Cumulus Clouds," *Tellus*, Vol. 11, No. 2, Stockholm, Sweden, May **1959**, pp. 202–215.

Eveson, G. F., Hall, E. W., and Ward, S. G., "Interaction Between Two Equal-Sized Equal-Settling Spheres Moving Through a Viscous Liquid," *British Journal of Applied Physics*, Vol. 10, No. 1, Institute of Physics, London, England, Jan. **1959**, pp. 43–47.

Fletcher, Neville Horner, *The Physics of Rainclouds*, Cambridge University Press, London, England, **1962**, 386 pp.

Golovin, A. M., "The Solution of an Equation for Cloud Droplet Coagulation in an Ascending Air Current," *Bulletin of the Academy of Science of U.S.S.R., Geophysical Series* No. 5, Akademiia Nauk, S.S.S.R., May **1963**, pp. 783–791.

Gunn, K. L. S., and Marshall, J. S., "The Distribution With Size of Aggregate Snowflakes," *Journal of Meteorology*, Vol. 15, No. 5, Oct. **1958**, pp. 452–461.

Happel, J., and Pfeffer, R., "The Motion of Two Spheres Following Each Other in a Viscous Fluid," *American Institute of Chemical Engineering Journal*, Vol. 6, No. 1, American Institute of Chemical Engineers, New York, N.Y., Mar. **1960**, pp. 129–133.

Hobbs, Peter V., "Ice Multiplication in Clouds," *Journal of the Atmospheric Sciences*, Vol. 26, No. 2, Mar. **1969**, pp. 315–318.

Hocking, L. M., "The Collision Efficiency of Small Drops," *Quarterly Journal of the Royal Meteorological Society*, Vol. 85, No. 363, London, England, Jan. **1959**, pp. 44–50

Hocking, L. M., and Jonas, P. R., "The Collision Efficiency of Small Drops," *Quarterly Journal of the Royal Meteorological Society*, Vol. 96, No. 410, London, England, Oct. **1970**, pp. 722–729.

Hosler, Charles L., and Hallgren, Richard E., "The Aggregation of Small Ice Crystals," *The Physical Chemistry of Aerosols*, Aberdeen University Press, Ltd., Aberdeen, Scotland, **1960**, pp. 200–207.

Howell, Wallace E., "The Growth of Cloud Drops in Uniformly Cooled Air," *Journal of Meteorology*, Vol. 6, No. 2, Apr. **1949**, pp. 134–149.

Kessler, Edwin, "On the Continuity of Water Substance," *ESSA Technical Memorandum* IERTM-NSSL 33, National Severe Storms Laboratory, Norman, Okla., Apr. **1967**, 125 pp.

Kessler, Edwin, "On the Distribution and Continuity of Water Substance in Atmospheric Circulation," *Meteorological Monographs*, Vol. 10, No. 32, American Meteorological Society, Boston, Mass., Nov. **1969**, 84 pp.

Koenig, L. Randall, "The Glaciating Behavior of Small Cumulonimbus Clouds," *Journal of the Atmospheric Sciences*, Vol. 20, No. 1, Jan. **1963**, pp. 29–47.

Kovetz, A., and Olund, B., "The Effect of Coalescence and Condensation on Rain Formation in a Cloud of Finite Vertical Extent," *Journal of the Atmospheric Sciences*, Vol. 26, No. 5, Part 2, Sept. **1969**, pp. 1060–1065.

Kraichnan, R. H., "Inertial Ranges in Two-Dimensional Turbulence," *Physics of Fluids*, Vol. 10, No. 7, July **1967**, pp. 1417–1423.

Langham, E. J., and Mason, B. J., "The Heterogeneous and Homogeneous Nucleation of Supercooled Water," *Proceedings of the Royal Society of London*, Vol. 247, No. 1251, England, Oct. 21, **1958**, pp. 493–504.

Langmuir, Irving, "The Production of Rain by a Chain Reaction in Cumulus Clouds at Temperatures Above Freezing," *Journal of Meteorology*, Vol. 5, No. 5, Oct. **1948**, pp. 175–192.

Leith, C. E., "Diffusion Approximation for Two-Dimensional Turbulence," *Physics of Fluids*, Vol. 11, No. 3, Mar. **1968**, pp. 671–673.

Lilly, D., "Numerical Simulation of Two-Dimensional Turbulence," *Physics of Fluids Supplement II*, Vol. 12, American Institute of Physics, New York, N.Y., **1969**, pp. II–240—249.

Liu, J. Y., and Orville, H. D., "Numerical Modeling of Precipitation and Cloud Shadow Effects on Mountain-Induced Cumuli," *Journal of the Atmospheric Sciences*, Vol. 26, No. 6, Nov. **1969**, pp. 1283–1298.

Marshall, J. S., and Palmer, W. McK., "The Distribution of Raindrops with Size," *Journal of Meteorology*, Vol. 5, No. 4, Aug. **1948**, pp. 165–166.

Mason, Basil John, "On the Melting of Hailstones," *Quarterly Journal of the Royal Meteorological Society*, Vol. 82, No. 352, London, England, Apr. **1956**, pp. 209–216.

Mason, Basil John, *The Physics of Clouds*, Clarendon Press, Oxford, England, **1957**, 481 pp. (see p. 186).

Mason, Basil John, "Some Outstanding Problems in Cloud Physics—The Interaction of Microphysical and Dynamical Processes," *Quarterly Journal of the Royal Meteorological Society*, Vol. 95, No. 405, London, England, July **1969**, pp. 449–485.

Molenkamp, Charles R., "Accuracy of Finite-Difference Methods Applied to the Advection Equation," *Journal of Applied Meteorology*, Vol. 7, No. 2, Apr. **1968**, pp. 160–167.

Morton, B. R., "The Ascent of Turbulent Forced Plumes in a Calm Atmosphere," *International Journal of Air Pollution*, Vol. 1, No. 3, New York, N.Y., Jan. **1959**, pp. 184–197.

Mossop, S. C., "Comparisons Between Concentration of Ice Crystals in Cloud and the Concentration of Ice Nuclei," *Journal de Recherches Atmosphériques*, Vol. 3, No. 1/2, Clermont-Ferrand, Lannemezan, France, Jan./June **1968**, pp. 119–124.

Mossop, S. C., and Ono, A., "Measurements of Ice Crystal Concentration in Clouds," *Journal of the Atmospheric Sciences*, Vol. 26, No. 1, Jan. **1969**, pp. 130–137.

Murray, F. W., "Numerical Models of a Tropical Cumulus Cloud With Bilateral and Axial Symmetry," *Monthly Weather Review*, Vol. 98, No. 1, Jan. **1970**, pp. 14–28.

Ogura, Yoshimitsu, "A Review of Numerical Modeling Research on Small Scale Convection in the Atmosphere," *Meteorological Monographs*, Vol. 5, No. 27, American Meteorological Society, Boston, Mass., Sept. **1963***a*, pp. 65–76.

Ogura, Yoshimitsu, "The Evolution of a Moist Convective Element in a Shallow, Conditionally Unstable Atmosphere: A Numerical Calculation," *Journal of the Atmospheric Sciences*, Vol. 20, No. 5, Sept. **1963***b*, pp. 407–424.

Ogura, Yoshimitsu, and Phillips, Norman A., "Scale Analysis of Deep and Shallow Convection in the Atmosphere," *Journal of the Atmospheric Sciences*, Vol. 19, No. 2, Mar. **1962**, pp. 173–179.

Orville, Harold D., "A Numerical Study of the Initiation of Cumulus Clouds Over Mountainous Terrain," *Journal of the Atmospheric Sciences*, Vol. 22, No. 6, Nov. **1965**, pp. 684–699.

Orville, Harold D., "Ambient Wind Effects on the Initiation and Development of Cumulus Clouds Over Mountains," *Journal of the Atmospheric Sciences*, Vol. 25, No. 3, May **1968**, pp. 385–403.

Orville, Harold D., and Sloan, Lansing J., "A Numerical Simulation of the Life History of a Rainstorm," *Journal of the Atmospheric Sciences*, Vol. 27, No. 8, Nov. **1970**, pp. 1148–1159.

Rand Corporation, Weather Modification Research Project Staff, "Weather-Modification Progress and the Need for Interactive Research," *Bulletin of the American Meteorological Society*, Vol. 50, No. 4, Apr. **1969**, pp. 216–246.

Ricou, Francis P., and Spalding, D. B., "Measurements of Entrainment by Axisymmetrical Turbulent Jets," *Journal of Fluid Mechanics*, Vol. 11, Part 1, Cambridge University Press, Cambridge, England, Aug. **1961**, pp. 21–32.

Sartor, J. D., "The Role of Particle Interactions in the Distribution of Electricity in Thunderstorms," *Journal of the Atmospheric Sciences*, Vol. 24, No. 6, Nov. **1967**, pp. 601–615.

Schotland, R. M., "The Collision Efficiency of Cloud Drops of Equal Size," *Journal of Meteorology*, Vol. 14, No. 5, Oct. **1957**, pp. 381–385.

Semonin, R. G., and Plumlee, H. R., "Collision Efficiency of Charged Cloud Droplets in Electric Fields," *Journal of Geophysical Research*, Vol. 71, No. 18, Sept. 15, **1966**, pp. 4271–4278.

Shafrir, Uri, and Neiburger, Morris, "Collision Efficiencies of Two Spheres Falling in a Viscous Medium," *Journal of Geophysical Research*, Vol. 68, No. 13, July 1, **1963**, pp. 4141–4148.

Simpson, Joanne, "On Cumulus Entrainment and One-Dimensional Models," *Journal of the Atmospheric Sciences*, Vol. 28, No. 3, Apr. **1971**, pp. 449–455.

Simpson, Joanne, Simpson, Robert H., Andrews, Donald A., and Eaton, Max A., "Experimental Cumulus Dynamics." *Reviews of Geophysics*, Vol. 3, No. 3, Aug. **1965**, pp. 387–431.

Simpson, Joanne, and Wiggert, Victor, "Models of Precipitating Cumulus Towers," *Monthly Weather Review*, Vol. 97, No. 7, July **1969**, pp. 471–489.

Simpson, Joanne, and Wiggert, Victor, "1968 Florida Cumulus Seeding Experiment: Numerical Model Results," *Monthly Weather Review*, Vol. 99, No. 2, Feb. **1971**, pp. 87–118.

Squires, P., "The Spatial Variation of Liquid Water and Droplet Concentration in Cumuli," *Tellus*, Vol. 10, No. 3, Stockholm, Sweden, Aug. **1958**, pp. 372–380.

Squires, P., and Turner, J. S., "An Entraining Jet Model for Cumulo-Nimbus Updraughts," *Tellus*, Vol. 14, No. 4, Stockholm, Sweden, Nov. **1962**, pp. 422–434

Srivastava, R. C., "A Study of the Effect of Precipitation on Cumulus Dynamics," *Journal of the Atmospheric Sciences*, Vol. 24, No. 1, Jan. **1967**, pp. 36–45.

Steinberger, E. H., Pruppacher, H.R., and Neiburger, M., "On the Hydrodynamics of Pairs of Spheres Falling Along Their Line of Centers in a Viscous Medium," *Journal of Fluid Mechanics*, Vol. 34, Part 4, Cambridge University Press, London, England, Dec. **1968**, pp. 809–819.

Takeda, Takao, "The Downdraft in the Convective Cloud and Raindrops: A Numerical Computation," *Journal of the Meteorological Society of Japan*, Ser. 2, Vol. 44, No. 1, Tokyo, Feb. **1966***a*, pp. 1–11.

Takeda, Takao, "Effects of the Prevailing Wind With Vertical Shear on the Convective Cloud Accompanied With Heavy Rainfall," *Journal of the Meteorological Society of Japan*, Ser. 2, Vol. 44, No. 2, Tokyo, Apr. **1966***b*, pp. 129–144.

Takeda, Takao, "Numerical Simulation of a Precipitating Convective Cloud: The Formation of a 'Long-Lasting' Cloud," *Journal of the Atmospheric Sciences*, Vol. 28, No. 3, Apr. **1971**, pp. 350–376.

Telford, J. W., Thorndike, N. S., and Bowen, E. G., "The Coalescence Between Small Water Drops," *Quarterly Journal of the Royal Meteorological Society*, Vol. 81, No. 348, London, England, Apr. **1955**, pp. 241–250.

Twomey, S., "Computations of Rain Formation by Coalescence," *Journal of the Atmospheric Sciences*, Vol. 23, No. 4, July **1966**, pp. 405–411.

Warner, J., "The Water Content of Cumuliform Cloud," *Tellus*, Vol. 7, No. 4, Stockholm, Sweden, Nov. **1955**, pp. 449–457,

Warner, J., "The Microstructure of Cumulus Cloud: Part I. General Features of the Droplet Spectrum," *Journal of the Atmospheric Sciences*, Vol. 26, No. 5, Part 2, Sept. **1969**, pp. 1049–1059.

Warner, J., "On Steady-State One-Dimensional Models of Cumulus Convection," *Journal of the Atmospheric Sciences*, Vol. 27, No. 7, Oct. **1970**, pp. 1035–1040.

Warshaw, Michael, "Cloud Droplet Coalescence: Statistical Foundations and a One-Dimensional Sedimentation Model," *Journal of the Atmospheric Sciences*, Vol. 24, No. 3, May **1967**, pp. 278–286.

Weickmann, Helmut K., *Artificial Stimulation of Rain*, Pergamon Press, New York, N.Y., **1957**, 427 pp. (see pp. 161–166).

Weickmann, Helmut K., "Progress in Hailstorm Research," *ESSA Technical Report*, ERL 129–APCL 7, Atmospheric Physics and Chemistry Laboratory, Boulder, Colo., May **1969**, 21 pp.

Weickmann, Helmut K., and aufm Kampe, H. J., "Physical Properties of Cumulus Clouds," *Journal of Meteorology*, Vol. 10, No. 3, June **1953**, pp. 204–211.

Weinstein, Alan I., "A Numerical Model of Cumulus Dynamics and Microphysics," *Journal of the Atmospheric Sciences*, Vol. 27, No. 2, Mar. **1970**, pp. 246–255.

WMO–ICSU Joint Organizing Committee, "The Planning of GARP Tropical Experiments," *GARP Publications Series*, No. 4, Jan. **1970**, pp. 1–78.

Woods, J. D., and Mason, B. J., "The Wake Capture of Water Drops in Air," *Quarterly Journal of the Royal Meteorological Society*, Vol. 91, No. 387, London, England, Jan. **1965**, pp. 35–43.

Woodward, Betsy, "The Motion in and Around Isolated Thermals," *Quarterly Journal of the Royal Meteorological Society*, Vol. 85, No. 364, London, England, Apr. **1959**, pp. 144–151.

[*Received August 17, 1970; revised July 19, 1971*]

449-617 O - 72 - 3